

N 73 - 28888

IFSM-73-40

FRAC-  
TURE  
MECHANICS  
INSTRUMENTATION

# LEHIGH UNIVERSITY



BONDED HALF PLANES CONTAINING  
AN ARBITRARILY ORIENTED CRACK.

By

## CASE FILE COPY

F. ERDOGAN  
AND  
O. AKSOGAN

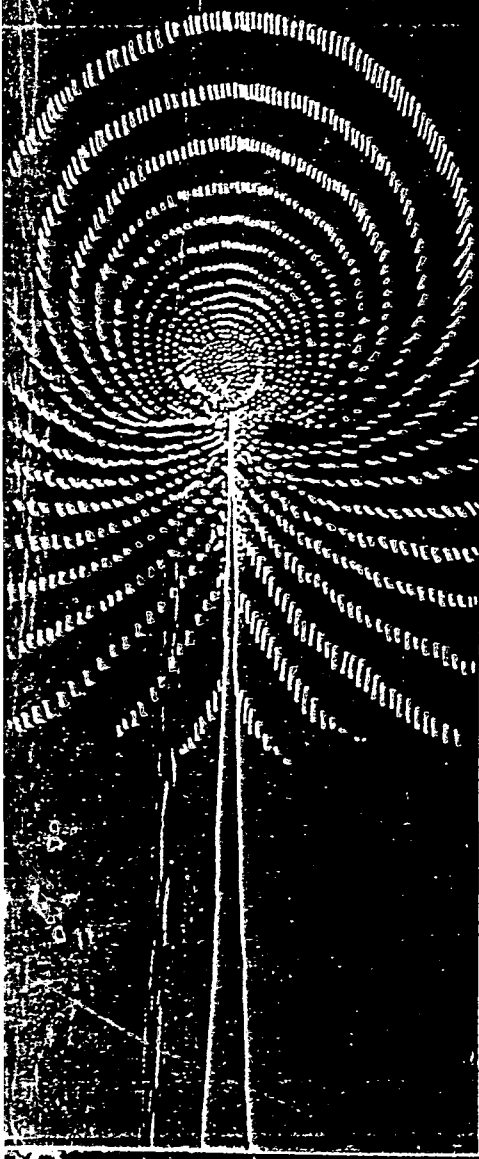
TECHNICAL REPORT NASA TR-73-9



MAY 1973

NATIONAL AERONAUTICS AND SPACE ADMINISTRATION

GRANT NGR-39-007-011



BONDED HALF PLANES CONTAINING  
AN ARBITRARILY ORIENTED CRACK\*

by

F. Erdogan and O. Aksogan\*\*  
Lehigh University, Bethlehem, Pa.

Abstract

The plane elastostatic problem for two bonded half planes containing an arbitrarily oriented crack in the neighborhood of the interface is considered. Using Mellin Transforms, the problem is formulated as a system of singular integral equations. The equations are solved for various crack orientations, material combinations, and external loads. The numerical results given in the paper include the stress intensity factors, the strain energy release rates, and the probable cleavage angles giving the direction of crack propagation.

1. INTRODUCTION

The structural strength of composite materials is controlled to a considerable extent by the size, shape, orientation, and distribution of the flaws and imperfections which exist in the material. Usually these flaws and imperfections exhibit themselves in the form of entrapped gas or weak impurities on the interface, ruptured bonds, cracks, inclusions, and geometric singularities arising from the particular shape of the constituent materials. From the viewpoint of fracture initiation and

---

\* This work was supported by NASA-Langley under The Grant NGR 39-007-011 and by The National Science Foundation under The Grant GK-11977.

\*\* Present Address: Middle East Technical University, Ankara, Turkey.

propagation in the medium particularly important are the manufacturing flaws such as flat cavities which develop during bonding or casting, small cracks resulting from the residual stresses, and fatigue cracks caused by the cyclic nature of the external loads. Thus, in studies relating to the fracture initiation and propagation in the material, it is necessary to have a good estimate of those factors representing the severity of the external loads in the neighborhood of the "isolated dominant flaw". Generally, the comparison of these factors (such as the stress intensity factors, the strain energy release rate, the crack opening stretch, or the cleavage stress at a characteristic distance from the flaw boundary) with the corresponding characteristic constant representing the resistance of the material to fracture constitutes the fracture criterion. If the dominant imperfection is completely imbedded in a homogeneous phase and is located sufficiently far from the phase boundaries or interfaces, then the disturbance of the stress field around the imperfection will not be affected by the neighboring phases and the disturbed stress field may be obtained by solving the problem for an infinite homogeneous solid. On the other hand if the flaw is located near a phase boundary or a bi-material interface, then the solution of the problem for the nonhomogeneous medium becomes necessary.

An up-to-date review of the available solutions for variety of crack and inclusion geometries in composite materials may be found in [1]. The primary interest of this paper is in the evaluation of the disturbed stress field around a crack located

near a bi-material interface or, as a limiting special case, free boundary. The problem was studied in a previous series of papers for two special crack orientations, namely the case of a crack located parallel to or at the interface [2-6] and the problem of a crack perpendicular to and crossing the interface [7, 8]. In this paper we will assume that the orientation of the crack with respect to the interface (i.e., the angle  $\theta_0$  and the distance  $d$  in Figure 1) is arbitrary and the problem is one of plane strain or generalized plane stress. As in the previous studies it will also be assumed that the interface in the non-homogeneous medium is either a plane or has a sufficiently large radius of curvature so that the disturbed stress field can be approximated by that of a crack in two bonded elastic half planes (Figure 1). Even though the problem will be formulated and solved for the bonded half planes, the technique described in the paper appears to be quite general and may be used to treat the problem of any number of bonded wedges with radial cracks.

## 2. THE INTEGRAL EQUATIONS OF THE PROBLEM

Using the conventional superposition technique the solution of the problem of a traction-free crack in the composite medium under a given set of external loads can be expressed as the sum of two solutions: the first obtained for the given external loads and the given medium without the crack, and the second obtained for the two bonded half planes with a crack where the only external loads are the crack surface tractions which are equal and opposite to the stresses found in the first solution on the

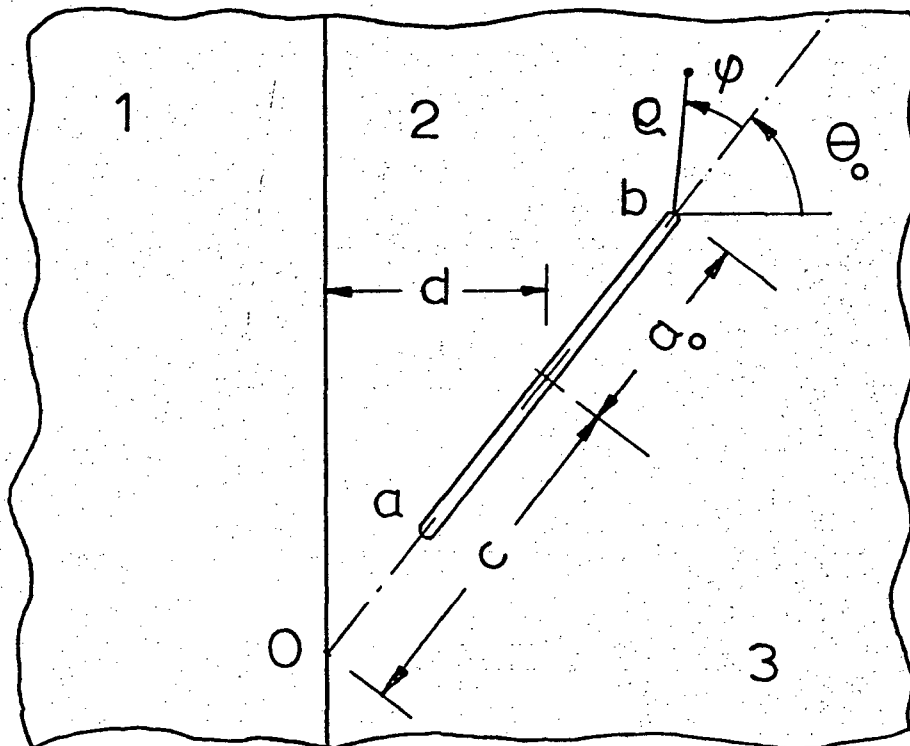


Figure 1. Notation for the inclined crack.

presumed location of the crack. It is clear that only the second solution which gives the disturbed stress field due to the existence of the crack will have singularities. Also note that in the second problem, since the external loads are local and statically self-equilibrating, in the application of Mellin transforms the regularity conditions required of the solution as  $r \rightarrow \infty$  will be satisfied. Following now, for example [9], in polar coordinates the plane elasticity problem for a medium having the elastic constants  $\mu$  and  $\kappa$  ( $\kappa = 3-4\nu$  for plane strain,  $\kappa = (3-\nu)/(1+\nu)$  for plane stress) may be formulated as

$$\sigma(r, \theta) = \tau_{r\theta} + i\tau_{\theta\theta} = -\frac{\partial}{\partial r} \left( \frac{1}{r} \frac{\partial \chi}{\partial \theta} \right) + i \frac{\partial^2 \chi}{\partial r^2},$$

$$\tau_{rr} = \frac{1}{r^2} \frac{\partial^2 \chi}{\partial \theta^2} + \frac{1}{r} \frac{\partial \chi}{\partial r},$$

$$\begin{aligned} v(r, \theta) = \frac{\partial u_r}{\partial r} + i \frac{\partial u_\theta}{\partial r} = \frac{1}{2\mu} \left\{ -\frac{\partial^2 \chi}{\partial r^2} + \frac{i}{r^2} \frac{\partial \chi}{\partial \theta} - \frac{i}{r} \frac{\partial^2 \chi}{\partial r \partial \theta} \right. \\ \left. + \frac{1+\kappa}{4} \left[ \frac{\partial \psi}{\partial \theta} + 2ir \frac{\partial \psi}{\partial r} + r \frac{\partial^2 \psi}{\partial r \partial \theta} + ir^2 \frac{\partial^2 \psi}{\partial r^2} \right] \right\}, \quad (1.a-c) \end{aligned}$$

$$\nabla^4 \chi = 0, \quad \nabla^2 \psi = 0, \quad \frac{\partial}{\partial r} \left( r \frac{\partial \psi}{\partial r} \right) = \nabla^2 \chi. \quad (2.a-c)$$

Referring to Figure 1, the medium will be considered as consisting of three infinite wedges: 1 ( $\mu_1, \kappa_1$ ),  $\frac{\pi}{2} < \theta < \frac{3\pi}{2}$ ; 2 ( $\mu_2, \kappa_2$ ),  $\theta_0 < \theta < \frac{\pi}{2}$ ; 3 ( $\mu_2, \kappa_2$ ),  $-\frac{\pi}{2} < \theta < \theta_0$ . For an infinite wedge with an arbitrary angle, using the Mellin transforms to solve (2), from (1) we obtain

$$\begin{aligned}
M[r^2\sigma, s] &= \Sigma(s, \theta) \\
&= 2i(s+1)[Ase^{is\theta} + B(s+1)e^{i(s+2)\theta} - \bar{B}e^{-i(s+2)\theta}] , \\
M[r^2\tau_{rr}, s] &= -s(s+1)(Ae^{is\theta} + \bar{A}e^{-is\theta}) \\
&\quad - (s+1)(s+4)[Be^{i(s+2)\theta} + \bar{B}e^{-i(s+2)\theta}] , \\
M[r^2v, s] &= V(s, \theta) \\
&= -\frac{s+1}{\mu} [Ase^{is\theta} + B(s+1)e^{i(s+2)\theta} + \kappa\bar{B}e^{-i(s+2)\theta}] , \\
\end{aligned} \tag{3.a-c}$$

where A and B are functions of the transform variable s. The Mellin transform of a function f(r) defined and suitably regular in  $(0 < r < \infty)$ , and its inverse are defined by

$$\begin{aligned}
F(s) &= M[f, s] = \int_0^{\infty} f(r)r^{s-1}dr , \\
f(r) &= \frac{1}{2\pi i} \int_{c-i\infty}^{c+i\infty} F(s)r^{-s}ds , \\
\end{aligned} \tag{4.a,b}$$

where c is such that  $r^{c-1}f(r)$  is absolutely integrable in  $(0, \infty)$ . The transform of derivatives may be shown to be

$$\int_0^{\infty} r^n \frac{d^n f(r)}{dr^n} r^{s-1}dr = (-1)^n \frac{\Gamma(s+n)}{\Gamma(s)} F(s) , \tag{5}$$

provided

$$r^{s+m-1} \frac{d^{m-1}f}{dr^{m-1}} \rightarrow 0 \text{ as } r \rightarrow (0, \infty) , \quad (m=1, \dots, n). \tag{6}$$

In applications conditions (6) provide the information to determine the strip of regularity containing the line  $\text{Re}(s) = c$  in the inversion integral.\*

\* It should be noted that in working with Mellin transforms up to the inversion stage in the manipulations the transform variable

If we now let the subscripts 1,2,3 stand for the wedges shown in Figure 1, the problem must be solved under the following boundary conditions:

$$\begin{aligned} \sigma_1(r, \pi/2) &= \sigma_2(r, \pi/2), & (0 \leq r < \infty), \\ v_1(r, \pi/2) &= v_2(r, \pi/2), & (0 \leq r < \infty), \end{aligned} \quad (5.a,b)$$

$$\begin{aligned} \sigma_1(r, 3\pi/2) &= \sigma_3(r, -\pi/2), & (0 \leq r < \infty), \\ v_1(r, 3\pi/2) &= v_3(r, -\pi/2), & (0 \leq r < \infty), \end{aligned} \quad (6.a,b)$$

$$\sigma_2(r, \theta_0) = \sigma_3(r, \theta_0), \quad (0 \leq r < \infty), \quad (7)$$

$$\lim_{\theta \rightarrow \theta_0 + 0} \sigma_2(r, \theta) = p_2(r) + ip_1(r), \quad (a < r < b), \quad (8)$$

$$v_2(r, \theta_0) = v_3(r, \theta_0), \quad (0 \leq r < a, b < r < \infty), \quad (9)$$

$$\int_a^b [v_2(r, \theta_0) - v_3(r, \theta_0)] dr = 0. \quad (10)$$

where  $\sigma_j$  and  $v_j$ , ( $j=1,2,3$ ) are defined by (1),  $\mu_2 = \mu_3$ , and note that (9) and (10) correspond to the condition of displacement continuity outside the crack. In the solution of the problem as given by (3) there are six unknown (complex) functions  $A_j(s)$ ,  $B_j(s)$ , ( $j=1,2,3$ ) to be determined. The homogeneous conditions (5)-(7) provide five equations. The sixth equation is obtained from the mixed conditions given by (8) and (9). Thus, eliminating five of the unknown functions, the problem may be formulated

---

$s$  is treated as a real variable. The function  $F(s)$  is analytically extended into the complex plane from the real line when the inversion is evaluated. In the present problem, the complex notation in (1) and (3) is used only for convenience. Thus, for example, in separating the transforms of the stress components  $\tau_{r\theta}$  and  $\tau_{\theta\theta}$  in (3.a),  $s$  should be treated as real and  $A$  and  $B$  should be treated as complex quantities.

as a system of dual integral equations for two unknown real functions by using (8) and (9). However, a somewhat more direct method to solve the problem would be its reduction to a system of singular integral equations for a pair of real functions  $f_1$  and  $f_2$  defined by\*

$$v_2(r, \theta_0+0) - v_3(r, \theta_0-0) = f(r) = f_2(r) + if_1(r), \quad (a < r < b). \quad (11)$$

If (8) and (9) are replaced by

$$v_2(r, \theta_0) - v_3(r, \theta_0) = \begin{cases} f(r), & (a < r < b), \\ 0, & (0 \leq r < a, b < r < \infty), \end{cases} \quad (12)$$

and if we define

$$\begin{aligned} U(s) &= M[r^2 \{v_2(r, \theta_0) - v_3(r, \theta_0)\}, s] = \int_a^b f(r) r^{s+1} dr \\ &= \int_a^b [f_2(r) + if_1(r)] r^{s+1} dr = U_2(s) + iU_1(s), \end{aligned} \quad (13)$$

by substituting from (3) into (5)-(7) and (13) we obtain six linear algebraic equations in  $A_j$  and  $B_j$ , ( $j=1,2,3$ ), which may be solved giving  $A_j(s)$  and  $B_j(s)$  in terms of  $U(s)$ . For example, for the wedge 2 we find

$$\begin{aligned} A_2(s) &= \frac{\mu_2}{(1+\kappa_2)s(s+1)(e^{i\pi s} - e^{-i\pi s})} \{ [m_1(s+1)se^{is\theta_0} \\ &+ m_1(s+1)^2e^{i(s+2)\theta_0} - se^{-is(\pi+\theta_0)} + m_2e^{i(s+2)\theta_0}] U_2(s) \\ &+ [m_1(s+1)(s+2)e^{is\theta_0} + m_1(s+1)^2e^{i(s+2)\theta_0} \\ &+ (s+2)e^{-is(\pi+\theta_0)} + m_2e^{i(s+2)\theta_0}] iU_1(s) \}, \end{aligned}$$

\* Note that physically  $f_1$  and  $f_2$  represent the densities of edge dislocations distributed along  $\theta = \theta_0$  in two bonded half planes.

$$\begin{aligned}
B_2(s) = & \frac{\mu_2}{(1+\kappa_2)(s+1)(e^{-i\pi s} - e^{i\pi s})} \{ [-m_1 s e^{is\theta_0} \\
& - m_1(s+1)e^{i(s+2)\theta_0} - e^{-i(s\theta_0 + 2\theta_0 + s\pi)}] U_2(s) \\
& - [m_1(s+2)e^{is\theta_0} + m_1(s+1)e^{i(s+2)\theta_0} \\
& - e^{-i(s\theta_0 + 2\theta_0 + s\pi)}] i U_1(s) \}, \quad (14.a,b)
\end{aligned}$$

where

$$\begin{aligned}
m_1 &= (m-1)/(\kappa_2 m+1), \quad m = \mu_1/\mu_2, \\
m_2 &= (\kappa_1 - m\kappa_2)/(\kappa_1 + m). \quad (15)
\end{aligned}$$

Expressions similar to (14) may be found for wedges 1 and 3.

All the field quantities in wedge 2 may now be obtained in terms of  $f(r)$  by substituting from (14) into (3) and using the inversion formula. In particular, from (14), (3.a), (8), and (4.b) we obtain

$$\begin{aligned}
\frac{1+\kappa_2}{\mu_2} [p_2(r) + ip_1(r)] = & \lim_{\theta \rightarrow \theta_0 + 0} \frac{1}{\pi} \int_a^b [K_2(r, r_0, \theta) f_2(r_0) \\
& + iK_1(r, r_0, \theta) f_1(r_0)] dr_0, \quad (a < r < b), \quad (16)
\end{aligned}$$

$$\begin{aligned}
K_2(r, r_0, \theta) = & \int_{c-i\infty}^{c+i\infty} \frac{ds}{e^{i\pi s} - e^{-i\pi s}} \frac{r_0^{s+1}}{r^{s+2}} \{ m_1 s(s+1) e^{is(\theta+\theta_0)} \\
& + [m_2 + m_1(s+1)^2] e^{i(s\theta + s\theta_0 + 2\theta_0)} - s e^{is(\theta - \theta_0 - \pi)} \\
& + m_1 s(s+1) e^{i(s\theta + s\theta_0 + 2\theta)} + m_1(s+1)^2 e^{i(s+2)(\theta+\theta_0)} \\
& + (s+1) e^{i(s\theta + 2\theta - s\theta_0 - 2\theta_0 - s\pi)} \\
& + m_1 s e^{-i(s\theta + 2\theta + s\theta_0)} + m_1(s+1) e^{-i(s+2)(\theta+\theta_0)} \\
& + e^{i(s\theta_0 + 2\theta_0 - s\theta - 2\theta + s\pi)} \},
\end{aligned}$$

$$\begin{aligned}
K_1(r, r_0, \theta) = & \int_{c-i\infty}^{c+i\infty} \frac{ds}{e^{i\pi s} - e^{-i\pi s}} \frac{r_0^{s+1}}{r^{s+2}} \{ m_1(s+1)(s+2)e^{is(\theta+\theta_0)} \\
& + [m_2 + m_1(s+1)^2]e^{i(s\theta_0 + s\theta + 2\theta_0)} \\
& + (s+2)e^{is(\theta-\theta_0-\pi)} + m_1(s+1)(s+2)e^{i(s\theta + s\theta_0 + 2\theta)} \\
& + m_1(s+1)^2e^{i(s+2)(\theta+\theta_0)} \\
& - (s+1)e^{i(s\theta + 2\theta - s\theta_0 - 2\theta_0 - s\pi)} \\
& - m_1(s+2)e^{-i(s\theta + s\theta_0 + 2\theta)} - m_1(s+1)e^{-i(s+2)(\theta+\theta_0)} \\
& + e^{i(s\theta_0 + 2\theta_0 - s\theta - 2\theta + s\pi)} \} . \quad (17.a,b)
\end{aligned}$$

In (16) the order of integrations has been changed. For  $\theta > \theta_0$ , since the related integrals are uniformly convergent, this is permissible. (16) provide a system of integral equations to determine the unknown functions  $f_1$  and  $f_2$ . To solve this system the kernels  $K_1$  and  $K_2$  must be evaluated which may be done either by using the residue theory and expressing them as infinite series or by reducing the integrals to real integrals and evaluating them numerically. In either case, it is first necessary to determine the strip of regularity containing the constant  $c$ . Let the integrands in (17) be analytically extended into the entire plane and let the poles  $s_j$  be ordered as

$$--- < \text{Re}(s_{-2}) < \text{Re}(s_{-1}) < \text{Re}(s_{+1}) < \text{Re}(s_{+2}) < --- \quad (18)$$

Let  $\text{Re}(s_{-1}) < c < \text{Re}(s_{+1})$ . Thus, the integrals in (17) may be evaluated by closing the contour to the left for  $r < r_0$ , and to the right for  $r > r_0$  by means of semicircles of infinite radius, and by summing the residues. Noting that for  $r \rightarrow 0$ ,  $\tau_{ij} \sim O(r^{-\lambda})$ ,  $\text{Re}(\lambda) < 1$ , and for  $r \rightarrow \infty$ ,  $\tau_{ij} \sim O(r^{-\alpha})$ ,  $\text{Re}(\alpha) \geq 1$ , and since the

residues are of the form  $r^{-(s_j+2)}$ ,  $s_j$  then should be ordered such that

$$\operatorname{Re}(s_{-1}) < -1, \quad \operatorname{Re}(s_{+1}) \geq -1. \quad (19)$$

Thus,  $\operatorname{Re}(s_{-1}) < \operatorname{Re}(s) = c < -1$  gives the strip of regularity,  $s_{-1}$  being the first pole to the left of the line  $\operatorname{Re}(s) = -1$ .

For an arbitrary value of  $\theta_0$ , even though the residues in (17) may be evaluated without any difficulty, the resulting infinite series cannot be summed in closed form. Hence, it is difficult to study the singular behavior of the kernels. For this reason in this paper the kernels will be evaluated by reducing (17) to real integrals. For this we let  $c = -1$ ,  $s = -1 + iy$ ,  $(-\infty < y < \infty)$ , and indent the contour in such a way that the pole  $s_{+1} = -1$  lies to the right of the line of integration. The integrals in (17) may then be expressed as

$$\begin{aligned} K_k(r, r_0, \theta) &= \int_{c-i\infty}^{c+i\infty} H_k(s) ds \\ &= \int_{-\infty}^{\infty} H_k(-1+iy) idy - \lim_{s \rightarrow -1} \pi i (s+1) H_k(s), \end{aligned} \quad (k=1,2). \quad (20)$$

Evaluating the residue at  $s = -1$ , from (17) it may be shown that

$$\lim_{s \rightarrow -1} \pi i (s+1) H_k(s) = \frac{1}{r} (m_2 - m_1 - 2), \quad (k=1,2). \quad (21)$$

On the other hand, from (10) and (11) we have

$$\int_a^b f_k(r_0) dr_0 = 0, \quad (k=1,2). \quad (22)$$

Thus, when substituted into (16), the integrated terms in (20)

will have no contribution. In the remaining integral in (20) the integrand  $H_k$  turns out to be the sum of an odd function and an even function\* in  $y$ , giving  $K_j$  in terms of real integrals in  $(0, \infty)$ . As  $r \rightarrow r_0$  these integrals become divergent. Since the integrands are bounded at  $y=0$ , the divergent parts can be separated by considering the asymptotic behavior of the integrands as  $y \rightarrow \infty$ . By defining

$$\rho = \log(r_0/r), \quad \epsilon = \theta - \theta_0, \quad (23)$$

for small values of  $\epsilon$  from (17) and (20) it may be shown that

$$\begin{aligned} K_k(r, r_0, \epsilon) &= \frac{2}{r} \int_0^{\infty} \{e^{-\epsilon y} [1 + o(e^{-y(\pi-2\theta_0)})] \sin \rho y \\ &\quad + o(e^{-y(\pi-2\theta_0+\epsilon)}) \cos \rho y\} dy \\ &= \frac{2}{r} \frac{\rho}{\rho^2 + \epsilon^2} + M_k(r, r_0, \epsilon), \quad (0 \leq \theta_0 < \frac{\pi}{2}, k=1,2), \end{aligned} \quad (24)$$

where  $M_k(r, r_0, 0)$  is bounded for all values of  $r$  and  $r_0$  in the closed interval  $[a, b]$ .

Substituting now from (24) into (16), separating the real and imaginary parts, and letting  $\epsilon \rightarrow 0$  we obtain

$$\frac{1+\kappa_2}{2\mu_2} p_i(r) = \frac{1}{\pi} \int_a^b \sum_{j=1}^2 \left[ \frac{\delta_{ij}}{r \log(r_0/r)} + k_{ij}(r, r_0) \right] f_j(r_0) dr_0, \quad (i=1,2; a < r < b), \quad (25)$$

where the bounded kernels  $k_{ij}$ ,  $(i, j=1,2)$  are given by

$$\begin{aligned} k_{11}(r, r_0) &= \frac{1}{2r} \int_0^{\infty} \frac{dy}{\sinh \pi y} \sin \rho y [\cosh 2\theta_0 y (m_1 + 4m_1 y^2 \cos^2 \theta_0 - m_2) \\ &\quad + 2m_1 y \sin 2\theta_0 \sinh 2\theta_0 y + 2e^{-\pi y}], \end{aligned}$$

\* If not, it can always be put in that form.

$$k_{12}(r, r_0) = \frac{1}{2r} \int_0^{\infty} \frac{dy}{\sinh \pi y} [\cos \pi y \sinh 2\theta_0 y (4m_1 y^2 \cos^2 \theta_0 - m_1 - m_2) - 4m_1 y \cos^2 \theta_0 \sin \pi y \sinh 2\theta_0 y],$$

$$k_{21}(r, r_0) = \frac{1}{2r} \int_0^{\infty} \frac{dy}{\sinh \pi y} [\cos \pi y \sinh 2\theta_0 y (m_1 - 4m_1 y^2 \cos^2 \theta_0 + m_2) - 4m_1 y \cos^2 \theta_0 \sin \pi y \sinh 2\theta_0 y],$$

$$k_{22}(r, r_0) = \frac{1}{2r} \int_0^{\infty} \frac{dy}{\sinh \pi y} \sin \pi y [\cosh 2\theta_0 y (m_1 + 4m_1 y^2 \cos^2 \theta_0 - m_2) - 2m_1 y \sin 2\theta_0 \sinh 2\theta_0 y + 2e^{-\pi y}],$$

$$(a < (r, r_0) < b). \quad (26.a-d)$$

In the system of integral equations (25) the dominant kernels have a simple Cauchy-type singularity. This may be seen by observing that

$$\begin{aligned} \frac{1}{r \log(r_0/r)} &= \frac{1}{r \log[1 + (\frac{r_0}{r} - 1)]} \\ &= \frac{1}{r(\frac{r_0}{r} - 1)} \left[ 1 + \sum_{n=1}^{\infty} \frac{(-1)^n}{n+1} (\frac{r_0}{r} - 1)^{n-1} \right]^{-1} \\ &= \frac{1}{r_0 - r} [1 + o(\frac{r_0}{r} - 1)]. \end{aligned} \quad (27)$$

Thus, the system of singular integral equations is of the following conventional form:

$$\frac{1+\kappa_2}{2\mu_2} p_i(r) = \frac{1}{\pi} \int_a^b \sum_{j=1}^2 \left[ \frac{\delta_{ij}}{r_0 - r} + h_{ij}(r, r_0) \right] f_j(r_0) dr_0, \quad (i=1,2; a < r < b),$$

$$h_{ij}(r, r_0) = k_{ij}(r, r_0) + \left[ \frac{1}{r \log(r_0/r)} - \frac{1}{r_0 - r} \right] \delta_{ij}, \quad (i, j = 1, 2). \quad (28.a, b)$$

The index of the integral equations (28) is  $\kappa=1$ ; hence the solution will contain two arbitrary (real) constants which are determined from the additional conditions (22).

### 3. SOLUTION OF THE INTEGRAL EQUATIONS AND STRESS INTENSITY FACTORS

Referring to [10], it may be shown that the index of the system of singular integral equations is +1 and its solution is of the following form:

$$f_i(r) = g_i(r)[(b-r)(r-a)]^{-1/2}, \quad (a < r < b, i=1,2), \quad (29)$$

where the unknown functions  $g_i(r)$ , ( $i=1,2$ ) are bounded in the closed interval  $[a,b]$ . Even though, in principle, the system can be regularized and reduced to a pair of Fredholm-type integral equations, its solution may be obtained with much less computational effort by using the technique described in [11]. In the numerical solution the main problem is the evaluation of the kernels  $k_{ij}$  given by (26) for which in this paper a modified version of Filon's integration formula has been used [12].

In the application of the results to fracture problems in composites, of particular interest are the stress intensity factors and the probable plane of cleavage at a given crack tip. The normal and shear components,  $k_1$  and  $k_2$ , of the stress intensity factor are defined by and may be evaluated from the following expressions [2, 4, 5]:

$$k_1(a) = \lim_{r \rightarrow a} \sqrt{2(a-r)} \tau_{2\theta\theta}(r, \theta_0) = \lim_{r \rightarrow a} \frac{2\mu_2}{1+\kappa_2} \sqrt{2(r-a)} f_1(r),$$

$$\begin{aligned}
k_1(b) &= \lim_{r \rightarrow a} \sqrt{2(r-b)} \tau_{2\theta\theta}(r, \theta_0) = - \lim_{r \rightarrow b} \frac{2\mu_2}{1+\kappa_2} \sqrt{2(b-r)} f_1(r) , \\
k_2(a) &= \lim_{r \rightarrow a} \sqrt{2(a-r)} \tau_{2r\theta}(r, \theta_0) = \lim_{r \rightarrow a} \frac{2\mu_2}{1+\kappa_2} \sqrt{2(r-a)} f_2(r) , \\
k_2(b) &= \lim_{r \rightarrow b} \sqrt{2(r-b)} \tau_{2r\theta}(r, \theta_0) = - \lim_{r \rightarrow b} \frac{2\mu_2}{1+\kappa_2} \sqrt{2(b-r)} f_2(r) .
\end{aligned}
\tag{30.a-d}$$

The constants  $k_1$  and  $k_2$  are a measure of the intensity of the stresses around the crack tips. For example, at the crack tip ( $r=b, \theta=\theta_0$ ) the cleavage stress may be expressed as [13]

$$\sigma_{\phi\phi}(\rho, \phi) = \frac{1}{\sqrt{2\rho}} \cos \frac{\phi}{2} (k_1 \cos^2 \frac{\phi}{2} - \frac{3}{2} k_2 \sin \phi) + O(\sqrt{\rho}) , \tag{31}$$

where  $(\rho, \phi)$  are the polar coordinates at the crack tip,  $\phi$  being measured from the line which is the prolongation of the crack (Figure 1). Thus, once  $k_1$  and  $k_2$  are determined, for brittle solids the probable angle  $\phi_c$  of crack propagation may be postulated as the angle of the radial plane corresponding to the maximum cleavage stress and may be determined from  $\partial\sigma_{\phi\phi}/\partial\phi = 0$ , and  $\partial^2\sigma_{\phi\phi}/\partial\phi^2 < 0$ , or

$$k_2(1 - 3\cos\phi_c) - k_1\sin\phi_c = 0 ,$$

$$3k_2\sin\phi_c - k_1\cos\phi_c < 0 . \tag{32.a,b}$$

If an energy balance type criterion is used to estimate the crack propagation load, one may need to calculate the strain energy release rate which is given in terms of  $k_1$  and  $k_2$  as follows [13]:

$$\frac{\partial U}{\partial a_0} = \frac{\pi(1+\kappa)}{4\mu} (k_1^2 + k_2^2) , \quad (a_0 = (b-a)/2) . \tag{33}$$

#### 4. THE RESULTS

The material combinations, the external loads, and the geometrical configurations used in the numerical examples are summarized in Table 1 (see Figure 1 for the notation).

Table 1. The cases considered as numerical examples

	A		B		C		D		E		F	
	A <sub>1</sub>	A <sub>2</sub>	B <sub>1</sub>	B <sub>2</sub>	C <sub>1</sub>	C <sub>2</sub>	D <sub>1</sub>	D <sub>2</sub>	E <sub>1</sub>	E <sub>2</sub>	F <sub>1</sub>	F <sub>2</sub>
p <sub>1</sub> (r)	-p <sub>0</sub>	0	-p <sub>0</sub>	0								
p <sub>2</sub> (r)	0	-p <sub>0</sub>	0	-p <sub>0</sub>								
E <sub>1</sub> /E <sub>2</sub>	22.22		0.045			0	22.22		0			0
ν <sub>1</sub>	0.3		0.35				0.3					
ν <sub>2</sub>	0.35		0.3				0.35					
Fixed	d = 2a <sub>0</sub>		d = 2a <sub>0</sub>		d = 2a <sub>0</sub>		c = 2a <sub>0</sub>		c = 2a <sub>0</sub>		θ <sub>0</sub> = 40°	
Variab.	θ <sub>0</sub>		c									

The materials roughly correspond to a metal-hard polymer combination (say, aluminum-epoxy) (cases A, B, and D) and an elastic half plane (cases C, E, and F). The crack is along the line ( $\theta = \theta_0$ ,  $a < r < b$ ) and the distances  $c$ ,  $d$ , and the crack length  $2a_0$  are defined by (Figure 1)

$$2a_0 = b - a, \quad c = (a + b)/2, \quad d = c \cos \theta_0. \quad (34)$$

As indicated by Table 1, the results are obtained for uniform tractions

$$\tau_{2\theta\theta}(r, \theta_0) = p_1(r) = -p_0, \quad \tau_{2r\theta}(r, \theta_0) = 0, \quad \text{or}$$

$$p_1(r) = 0, \quad p_2(r) = -p_0, \quad (a < r < b) \quad (35.a,b)$$

applied to the crack surface. The results are given in Table 2. The quantities  $k_i^j$ , ( $i=1,2$ ) shown in the table are the stress intensity factor ratios defined by

$$k_i^j(c_j) = k_i(c_j)/(p_0\sqrt{a_0}), \quad (i,j=1,2; c_1=a, c_2=b) \quad (36)$$

where  $p_0\sqrt{a_0}$  is the stress intensity factor in a homogeneous infinite plane with a crack of length  $2a_0$ . The cleavage angle  $\phi_c$  given in the table was obtained from (32). All results are obtained for the plane strain case\* (i.e.,  $\kappa_j = 3-4\nu_j$ ,  $j=1,2$ ).

In cases A, B, and C the distance  $d$  from the interface is fixed as  $d = 2a_0$  and the crack angle  $\theta_0$  is varied (see Figure 1). The limiting cases  $\theta_0 = 0$  and  $\theta_0 = 90^\circ$  of this problem were given in [7] and [4] and were reproduced with the present computer program for verification. Note that if the crack is in the less stiff material (i.e.,  $E_1 > E_2$ , case A), generally there is a reduction, and if  $E_1 < E_2$  (case B and C) there is an increase in the stress intensity factors compared to the values for the homogeneous medium.

In cases D and E the radial distance  $c$  of the crack center is fixed as  $c = 2a_0$  and again  $\theta_0$  is varied. In case D where  $E_1/E_2 = 22.22$  for  $\theta_0 = \pi/2$  crack becomes an interface crack for which the closed form solution is given by (e.g., [2, 3]):

\* See [7] for the comparison of the plane strain and the plane stress results.

$$f_2(t) + if_1(t) = \frac{\sigma_0 - i\tau_0}{\mu_1 b_2 (1+\gamma)} (t - 2i\beta)R(t), \quad (|t| < 1),$$

$$(\tau_{2\theta_0} - i\tau_{2r\theta})_{\theta_0=\pi/2} = (\sigma_0 - i\tau_0)[(t - 2i\beta)R(t) - 1], \quad (|t| > 1),$$

$$R(t) = \left(\frac{t+1}{t-1}\right)^{i\beta} (t^2-1)^{-1/2}, \quad \beta = \frac{1}{2\pi} \log\left(\frac{1+\gamma}{1-\gamma}\right), \quad \gamma = b_1/b_2,$$

$$b_1 = \frac{\mu_2}{\mu_2 + \kappa_2 \mu_1} - \frac{\mu_2}{\mu_1 + \kappa_1 \mu_2}, \quad b_2 = \frac{\mu_2}{\mu_2 + \kappa_2 \mu_1} + \frac{\mu_2}{\mu_1 + \kappa_1 \mu_2},$$

$$t = (2r - b - a)/(b-a),$$

$$\begin{aligned} k_1 - ik_2 &= \lim_{r \rightarrow b+0} (\tau_{2\theta_0} - i\tau_{2r\theta})_{\theta_0=\pi/2} \left(\frac{r-b}{r-a}\right)^{i\beta} \sqrt{\frac{(r-a)(r-b)}{(b-a)/2}} \\ &= (\sigma_0 - i\tau_0)(1 - 2i\beta) \sqrt{(b-a)/2}, \end{aligned} \quad (37)$$

$$-(\sigma_0 + i\tau_0) = p_1(r) + ip_2(r),$$

where it should be noted that for the uniform tractions considered in (37) the stress intensity factors at  $r=a$  and  $r=b$  are the same. It is seen that in this case the stress singularity is oscillating in character and the definition of the stress intensity factors  $k_1$  and  $k_2$  is slightly different. Hence, at  $\theta_0 = \pi/2$  one would not expect the stress intensity factors and the cleavage angles to be continuous functions of  $\theta_0$ . The quantity which is expected to be continuous in  $\theta_0$  is the strain energy release rate given by (33) for a homogeneous medium. For the interface crack this quantity is given by [14]

$$\begin{aligned} \left(\frac{\partial U}{\partial a_0}\right)_{12} &= \frac{\pi}{2} \frac{(\mu_1 + \kappa_1 \mu_2)(\mu_2 + \kappa_2 \mu_1)}{\mu_1 \mu_2 [(1+\kappa_1)\mu_2 + (1+\kappa_2)\mu_1]} (k_1^2 + k_2^2)_{12} \\ &= \frac{\pi}{2} \frac{1 + \kappa_2}{\mu_2 a_{21}} (k_1^2 + k_2^2)_{12}. \end{aligned} \quad (38)$$

thus, for the crack imbedded in medium 2 if we evaluate the strain energy release rate ratio as

$$W_2 = \frac{4\mu_2}{\pi(1+\kappa_2)p_0^2 a_0} \left( \frac{\partial U}{\partial a_0} \right)_2 = k_1'^2 + k_2'^2, \quad (39)$$

from (38) and

$$\lim_{\theta_0 \rightarrow \pi/2} \left( \frac{\partial U}{\partial a_0} \right)_2 = \left( \frac{\partial U}{\partial a_0} \right)_{12} \quad (40)$$

we should have

$$\lim_{\theta_0 \rightarrow \pi/2} (k_1'^2 + k_2'^2) = \frac{2}{a_{21}} W_{21} = \frac{2}{a_{21}} \frac{k_1^2 + k_2^2}{p_0^2 a_0} = \frac{2}{a_{21}} (1 + \beta) \quad (41)$$

In case D,  $a_{21} = 3.93086$ ,  $\beta = 0.13420$  and the limit becomes  $W_2 \rightarrow 0.51796$  which is given in Table 2. If one plots  $W_2$  vs.  $\theta_0$  it may be seen that there is in fact a smooth transition from the imbedded crack to the interface crack.

In case E as  $\theta_0 \rightarrow \pi/2$  the crack approaches the traction-free surface; hence, as shown in the Table, the stress intensity factors tend to infinity. It should be pointed out that the analysis given in this paper is for a crack imbedded into a homogeneous medium. In the half plane problem for  $\theta_0 = \pi/2$  the crack disappears, there is a discontinuity in the solution, and hence the values given in the table for  $\theta_0 = \pi/2$  simply indicate the trend.

The results given for case F show the effect of the radial distance  $c$  (Figure 1) on the stress intensity factors  $k_i$  and the cleavage angle  $\phi_c$  for a fixed value of the crack angle,  $\theta_0 = 40^\circ$ . It is seen that as  $c$  increases the results approach the values corresponding to the infinite plane.

Table 2. The stress intensity factors and the probable crack propagation angles for the crack orientations, the material combinations, and the loads shown in Table 1. ( $k_i' = k_i/p_0\sqrt{a_0}$ ,  $i = 1, 2$ ,  $a_0 = (b-a)/2$ ).

Case	$\theta_0$	0	20°	40°	60°	80°	90°
A <sub>1</sub>	$k_1'(a)$	0.9349	0.9307	0.9216	0.9144	0.9143	0.9160
	$k_1'(b)$	0.9617	0.9572	0.9457	0.9318	0.9206	0.9160
	$k_2'(a)$	0	0.0025	0.00001	-0.0071	-0.0153	-0.0188
	$k_2'(b)$	0	0.0125	0.0209	0.0237	0.0215	0.0188
	$\phi_c(a)$	0	-0.306	-0.001	0.889	1.911	2.342
	$\phi_c(b)$	0	-1.492	-2.531	-2.915	-2.666	-2.342
A <sub>2</sub>	$k_1'(a)$	0	0.0223	0.0338	0.0333	0.0251	0.0191
	$k_1'(b)$	0	0.0030	0.0020	-0.0042	-0.0142	-0.0191
	$k_2'(a)$	0.9349	0.9395	0.9492	0.9580	0.9644	0.9663
	$k_2'(b)$	0.9617	0.9629	0.9655	0.9671	0.9672	0.9663
	$\phi_c(a)$	-70.53	-70.08	-69.85	-69.87	-70.03	-70.15
	$\phi_c(b)$	-70.53	-70.47	-70.49	-70.61	-70.81	-70.91
B <sub>1</sub>	$k_1'(a)$	1.0780	1.0929	1.1165	1.1389	1.1459	1.1420
	$k_1'(b)$	1.0464	1.0571	1.0796	1.1091	1.1344	1.1420
	$k_2'(a)$	0	-0.0098	-0.0077	-0.0062	0.0242	0.0321
	$k_2'(b)$	0	-0.0220	-0.0377	-0.0433	-0.0382	-0.0321
	$\phi_c(a)$	0	1.024	0.793	-0.623	-2.417	-3.210
	$\phi_c(b)$	0	2.384	3.985	4.462	3.852	3.210

Table 2 (cont.)

Case	$\theta_0$	0	20°	40°	60°	80°	90°
$B_2$	$k_1'(a)$	0	-0.0386	-0.0586	-0.0566	-0.0399	-0.0291
	$k_1'(b)$	0	-0.0082	-0.0092	-0.0002	0.0184	0.0291
	$k_2'(a)$	1.0780	1.0749	1.0590	1.0468	1.0400	1.0390
	$k_2'(b)$	1.0464	1.0465	1.0418	1.0385	1.0376	1.0390
	$\phi_c(a)$	-70.53	-71.22	-71.59	-71.56	-71.26	-71.06
	$\phi_c(b)$	-70.53	-70.68	-70.70	-70.53	-70.19	-70.00
$C_1$	$k_1'(a)$	1.0913	1.1049	1.1349	1.1604	1.1677	1.1621
	$k_1'(b)$	1.0539	1.0644	1.0918	1.1257	1.1543	1.1621
	$k_2'(a)$	0	-0.0114	-0.0093	0.0067	0.0276	0.0367
	$k_2'(b)$	0	-0.0251	-0.0431	-0.0498	-0.0439	-0.0367
	$\phi_c(a)$	0	1.184	0.941	-0.663	-2.703	-3.61
	$\phi_c(b)$	0	2.700	4.512	5.041	4.339	3.61
$C_2$	$k_1'(a)$	0	-0.0440	-0.0669	-0.0646	-0.0453	-0.0331
	$k_1'(b)$	0	-0.0095	-0.0109	-0.0003	0.0205	0.0331
	$k_2'(a)$	1.0913	1.0842	1.0686	1.0540	1.0452	1.0440
	$k_2'(b)$	1.0539	1.0523	1.0484	1.0444	1.0426	1.0440
	$\phi_c(a)$	-70.53	-71.31	-71.73	-71.70	-71.36	-71.05
	$\phi_c(b)$	-70.53	-70.70	-70.73	-70.54	-70.15	-69.93

Table 2 (cont.)

Case	$\theta_0$	0	20°	40°	60°	80°	90°
$D_1$	$k_1'(a)$	0.9349	0.9201	0.8749	0.8034	0.7334	
	$k_1'(b)$	0.9617	0.9523	0.9217	0.8631	0.7753	
	$k_2'(a)$	0	0.0018	-0.0093	-0.0539	-0.1297	
	$k_2'(b)$	0	0.0139	0.0319	0.0586	0.0960	
	$\phi_c(a)$	0	-0.227	1.221	7.608	18.96	
	$\phi_c(b)$	0	-1.670	-3.956	-7.701	-13.72	
	$W(a)$	0.8740	0.8465	0.7655	0.6484	0.5546	0.5180
	$W(b)$	0.9248	0.9070	0.8505	0.7483	0.6104	0.5180
$D_2$	$k_1'(a)$	0	0.0259	0.0608	0.1124	0.1547	
	$k_1'(b)$	0	0.0029	-0.0008	-0.0258	-0.0919	
	$k_2'(a)$	0.9349	0.9299	0.9160	0.8910	0.8012	
	$k_2'(b)$	0.9617	0.9586	0.9493	0.9305	0.8598	
	$\phi_c(a)$	-70.53	-70.00	-69.27	-68.14	-66.89	
	$\phi_c(b)$	-70.53	-70.47	-70.55	-71.06	-72.58	
	$W(a)$	0.8740	0.8654	0.8427	0.8064	0.6658	0.5180
	$W(b)$	0.9248	0.9188	0.9012	0.8664	0.7476	0.5180
$E_1$	$k_1'(a)$	1.0913	1.1222	1.2437	1.6218	4.0850	$\rightarrow \infty$
	$k_1'(b)$	1.0539	1.0725	1.1468	1.3871	3.0851	$\rightarrow \infty$
	$k_2'(a)$	0	-0.0121	-0.0041	0.1125	1.4986	$\rightarrow \infty$
	$k_2'(b)$	0	-0.0287	-0.0762	-0.2099	-1.2715	$\rightarrow -\infty$
	$\phi_c(a)$	0	1.235	0.373	-7.859	-33.458	
	$\phi_c(b)$	0	3.063	7.540	16.494	36.013	

Table 2 (cont.)

Case	$\theta_0$	0	20°	40°	60°	80°	90°
$E_2$	$k_1'(a)$	0	-0.0524	-0.1357	-0.3262	-0.9288	$\rightarrow -\infty$
	$k_1'(b)$	0	-0.0104	-0.0151	0.0056	0.1336	$\rightarrow \infty$
	$k_2'(a)$	1.0913	1.0979	1.1177	1.1381	1.2538	$\rightarrow \infty$
	$k_2'(b)$	1.0539	1.0589	1.0767	1.1187	1.2702	$\rightarrow \infty$
	$\phi_c(a)$	-70.53	-71.44	-72.86	-76.08	-84.91	
	$\phi_c(b)$	-70.53	-70.72	-70.80	-70.43	-68.53	
	$c/a_0$	1.1	1.2	1.4	1.6	2.0	4.0
$F_1$	$k_1'(a)$	2.5263	1.9959	1.5947	1.4150	1.2437	1.0543
	$k_1'(b)$	1.4694	1.3772	1.2764	1.2168	1.1468	1.0423
	$k_2'(a)$	0.2103	0.1091	0.0400	0.0141	-0.0041	-0.0073
	$k_2'(b)$	-0.2911	-0.2308	-0.1625	-0.1221	-0.0762	-0.0171
	$\phi_c(a)$	-9.388	-6.219	-2.870	-1.144	0.373	0.796
	$\phi_c(b)$	20.92	18.08	14.08	11.24	7.540	1.882
$F_2$	$k_1'(a)$	-1.0299	-0.6667	-0.3819	-0.2538	-0.1357	-0.0227
	$k_1'(b)$	-0.0716	-0.0491	-0.0300	-0.0219	-0.0151	-0.0066
	$k_2'(a)$	1.6185	1.4100	1.2580	1.1884	1.1177	1.0288
	$k_2'(b)$	1.2639	1.2054	1.1461	1.1134	1.0767	1.0227
	$\phi_c(a)$	-82.94	-79.73	-76.41	-74.65	-72.86	-70.95
	$\phi_c(b)$	-71.61	-71.31	-71.03	-70.91	-70.80	-70.65

The results given in Table 2 may be used to obtain the stress intensity factors in an arbitrarily loaded two-phase composite medium with an arbitrarily oriented crack provided the medium is loaded sufficiently far away from the crack region so that in the perturbed problem the crack surface tractions  $p_1(r)$  and  $p_2(r)$  can be approximated by uniform stresses. Thus if  $p_1(r) + ip_2(r) = p_1 + ip_2 = \text{constant}$ , we find

$$k_i(c_m) = -\sqrt{a_0} \sum_{j=1}^2 k'_{ij}(c_m) p_j, \quad (i, j, m = 1, 2; c_1 = a, c_2 = b) \quad (42)$$

where in  $k'_{ij}$   $i=1$  and  $i=2$  respectively correspond to the normal and the shear components of the stress intensity ratio given in Table 2 as  $k'_1$  and  $k'_2$ , and  $j=1$  and  $j=2$  respectively refer to the external loads  $p_1 \neq 0, p_2 = 0$  and  $p_1 = 0, p_2 \neq 0$ . For example, if the medium is loaded parallel to the interface away from the crack region, the uniform stresses in the uncracked material will be related by

$$\begin{aligned} \tau_{1r\theta}(r,0) &= \tau_{2r\theta}(r,0) = 0, \\ \frac{1-\nu_1^2}{E_1} \tau_{1\theta\theta}(r,0) &= \frac{1-\nu_2^2}{E_2} \tau_{2\theta\theta}(r,0), \\ \tau_{1\theta\theta}(r,0) &= \sigma_1, \quad \tau_{2\theta\theta}(r,0) = \sigma_2, \end{aligned} \quad (43)$$

where  $\sigma_1$  and  $\sigma_2$  are constant. In this case the stress intensity factors may be expressed as

$$\frac{k_1(c_m)}{\sigma_2 \sqrt{a_0}} = k'_1(c_m) = k'_{11}(c_m) \cos^2 \theta_0 + k'_{12}(c_m) \sin \theta_0 \cos \theta_0,$$

$$\frac{k_2(c_m)}{\sigma_2 \sqrt{a_0}} = k_2'(c_m) = k_{21}'(c_m) \cos^2 \theta_0 + k_{22}'(c_m) \sin \theta_0 \cos \theta_0, \quad (m=1,2; c_1=a, c_2=b). \quad (44)$$

Figures 2-9 show some of the results obtained from (44). Figures 2 and 3 give the results for the material combination and the crack orientation corresponding to case A in Table 1. Similarly, (aside from the external loads which are given by (43)), Figures 4 and 5 correspond to the case B, Figures 6 and 7 correspond to the case C, and Figures 8 and 9 correspond to the case D. Note that the probable cleavage angles  $\phi_c$  shown in Figures 3, 5, 7, and 9 are all negative and the direction of crack initiation is approximately perpendicular to the direction of the external load. The angle  $\phi_c = 70.53^\circ$  shown in the figures corresponds to the cleavage angle for an infinite plane containing a crack and subjected to a uniform shear at infinity parallel and perpendicular to the plane of the crack [13]. For a fixed external load, the figures clearly show the effect of the crack orientation on the stress intensity factors, and hence, on the fracture resistance of the composite medium.

#### REFERENCES:

1. F. Erdogan, "Fracture Problems in Composite Materials", J. Engng. Fracture Mechanics, Vol. 4, p. 811 (1972).
2. F. Erdogan and G. D. Gupta, "Stress Analysis of Multilayered Composites with a Flaw", Int. J. Solids Structures, Vol. 7, p. 39 (1971).
3. F. Erdogan and G. D. Gupta, "Layered Composites with an Interface Flaw", Int. J. Solids Structures, Vol. 7, p. 1089 (1971).

4. F. Erdogan, "Bonded Dissimilar Materials Containing a Crack Parallel to the Interface", J. Engng. Fracture Mechanics, Vol. 3, p. 231 (1971).
5. K. Arin and F. Erdogan, "Penny-Shaped Crack in an Elastic Layer Bonded to Dissimilar Half Spaces", Int. J. Engng. Sci., Vol. 9, p. 213 (1971).
6. F. Erdogan and K. Arin, "Penny-Shaped Interface Crack Between an Elastic Layer and a Half Space", Int. J. Engng. Sci., Vol. 10, p. 115 (1972).
7. T. S. Cook and F. Erdogan, "Stresses in Bonded Materials with a Crack Perpendicular to the Interface", Int. J. Engng. Sci., Vol. 10, p. 667 (1972).
8. F. Erdogan, V. Biricikoglu, "Two Bonded Half Planes with a Crack Going Through the Interface", to appear in Int. J. Engng. Sci. (1973).
9. E. G. Coker and L. G. N. Filon, A Treatise on Photoelasticity, Cambridge Univ. Press (1931).
10. N. I. Muskhelishvili, Singular Integral Equations, P. Noordhoff N. V. (1953).
11. F. Erdogan and G. D. Gupta, "On the Numerical Solution of Singular Integral Equations", Quarterly of Appl. Math., Vol. 29, p. 525 (1972).
12. M. Abramowitz and I. A. Stegun, Handbook of Mathematical Functions, Nat. Bureau of Standards Appl. Math. Series, 55 (1964).
13. F. Erdogan and G. C. Sih, "On the Crack Extension in Plates Under Plane Loading and Transverse Shear", J. Basic Engng., Trans. ASME, Vol. 85, Series D, p. 519 (1963).
14. B. M. Malyshev and R. L. Salganik, "The Strength of Adhesive Joints Using the Theory of Fracture", Int. J. Fracture Mechanics, Vol. 1, p. 114 (1965).

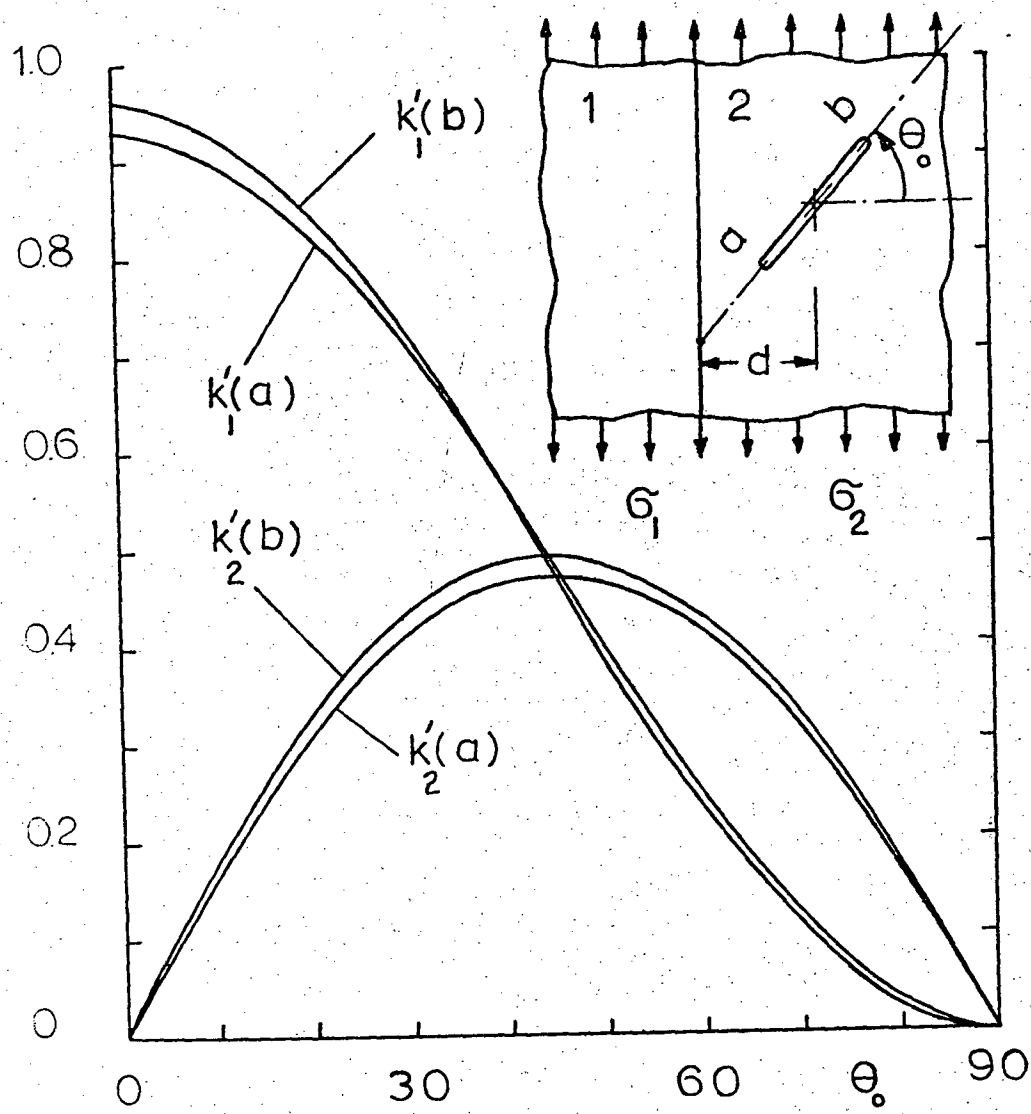


Figure 2. Stress intensity factor ratios in bonded half planes containing an arbitrarily oriented crack and loaded parallel to the interface ( $E_1/E_2 = 22.22$ ,  $\nu_1 = 0.3$ ,  $\nu_2 = 0.35$ ,  $d = 2a_0 = b - a = \text{constant}$ ).

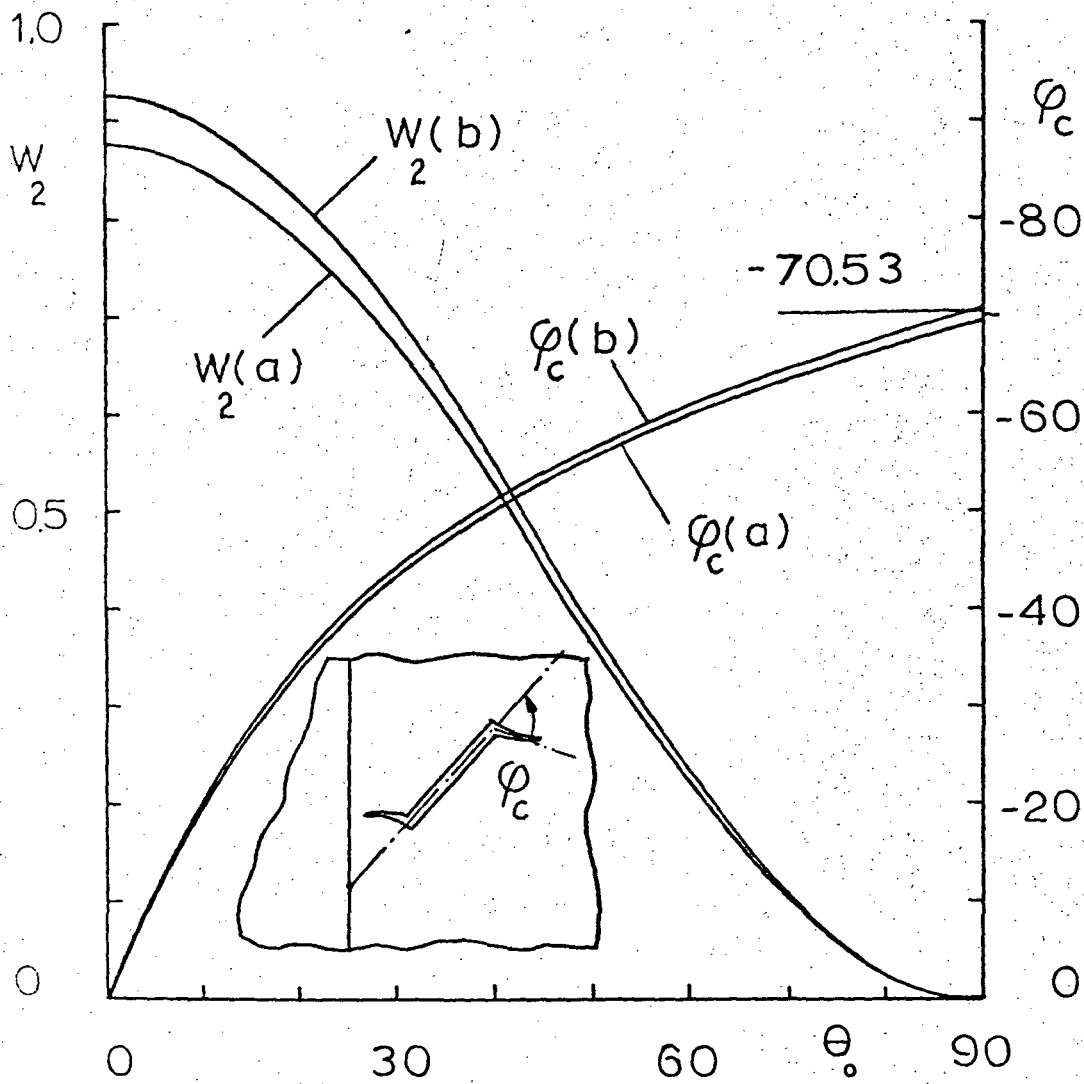


Figure 3. Cleavage angles and the strain energy release rates for the bonded planes shown in Figure 2 ( $E_1/E_2 = 22.22$ ,  $\nu_1 = 0.3$ ,  $\nu_2 = 0.35$ ,  $d = 2a_0 = b - a = \text{constant}$ ).

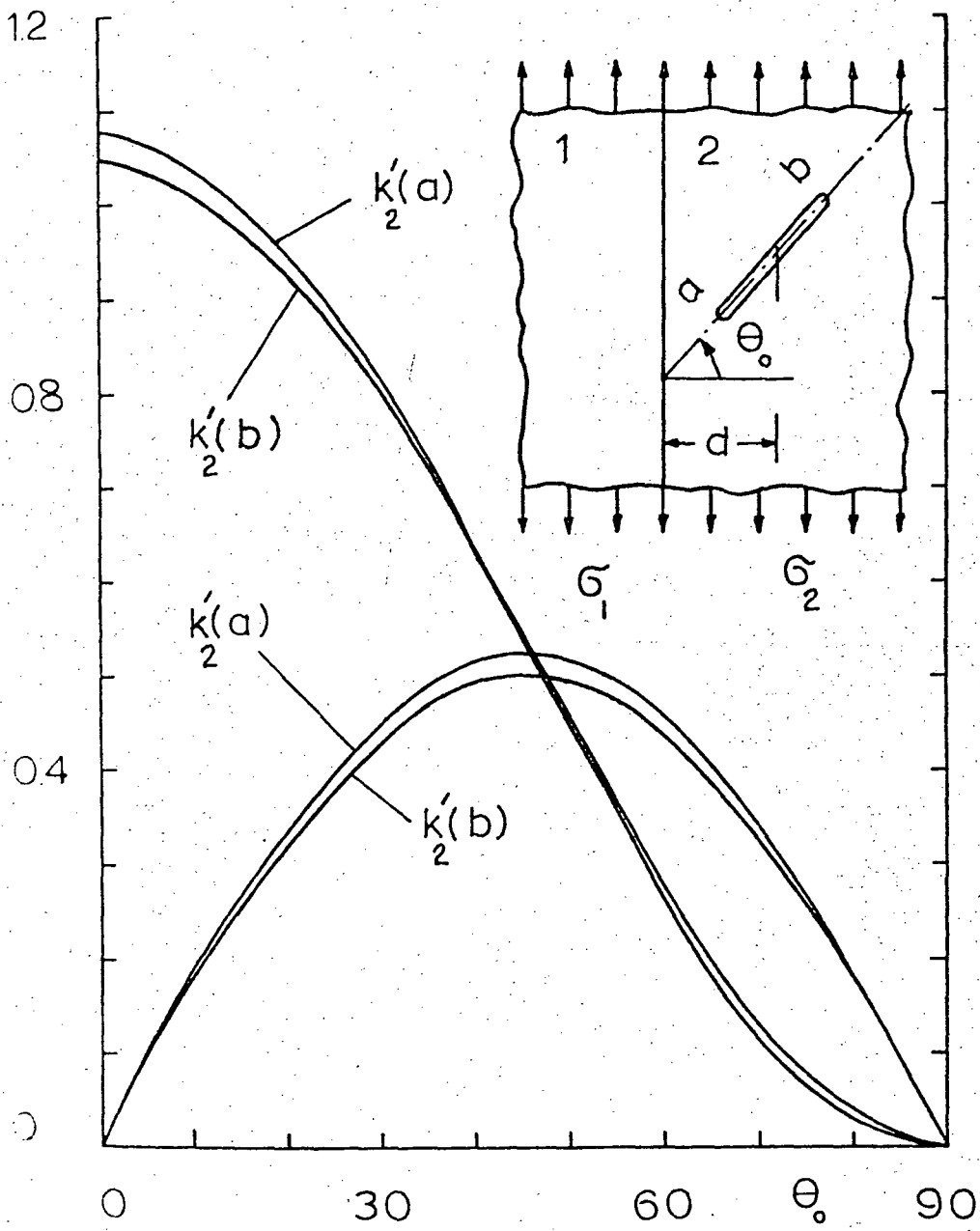


Figure 4. Stress intensity factor ratios in bonded half planes containing an arbitrarily oriented crack and loaded parallel to the interface ( $E_1/E_2 = 0.045$ ,  $\nu_1 = 0.35$ ,  $\nu_2 = 0.3$ ,  $d = 2a_0 = b - a =$  constant).

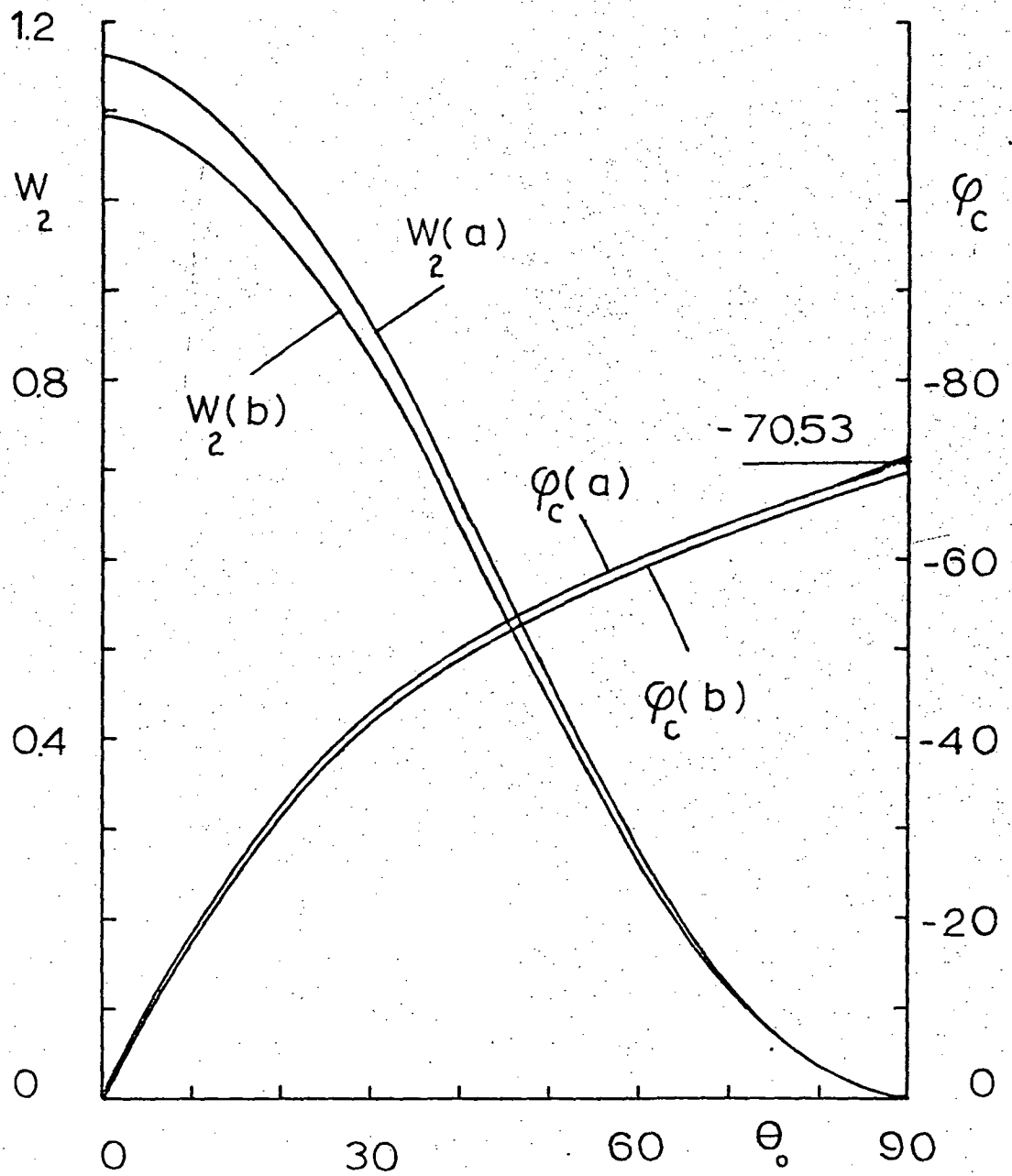


Figure 5. Cleavage angles  $\phi_c$  and the strain energy release rates  $W_2$  for the bonded planes shown in Figure 4 ( $E_1/E_2 = 0.045$ ,  $\nu_1 = 0.35$ ,  $\nu_2 = 0.3$ ,  $d = 2a_0 = b - a = \text{constant}$ ).

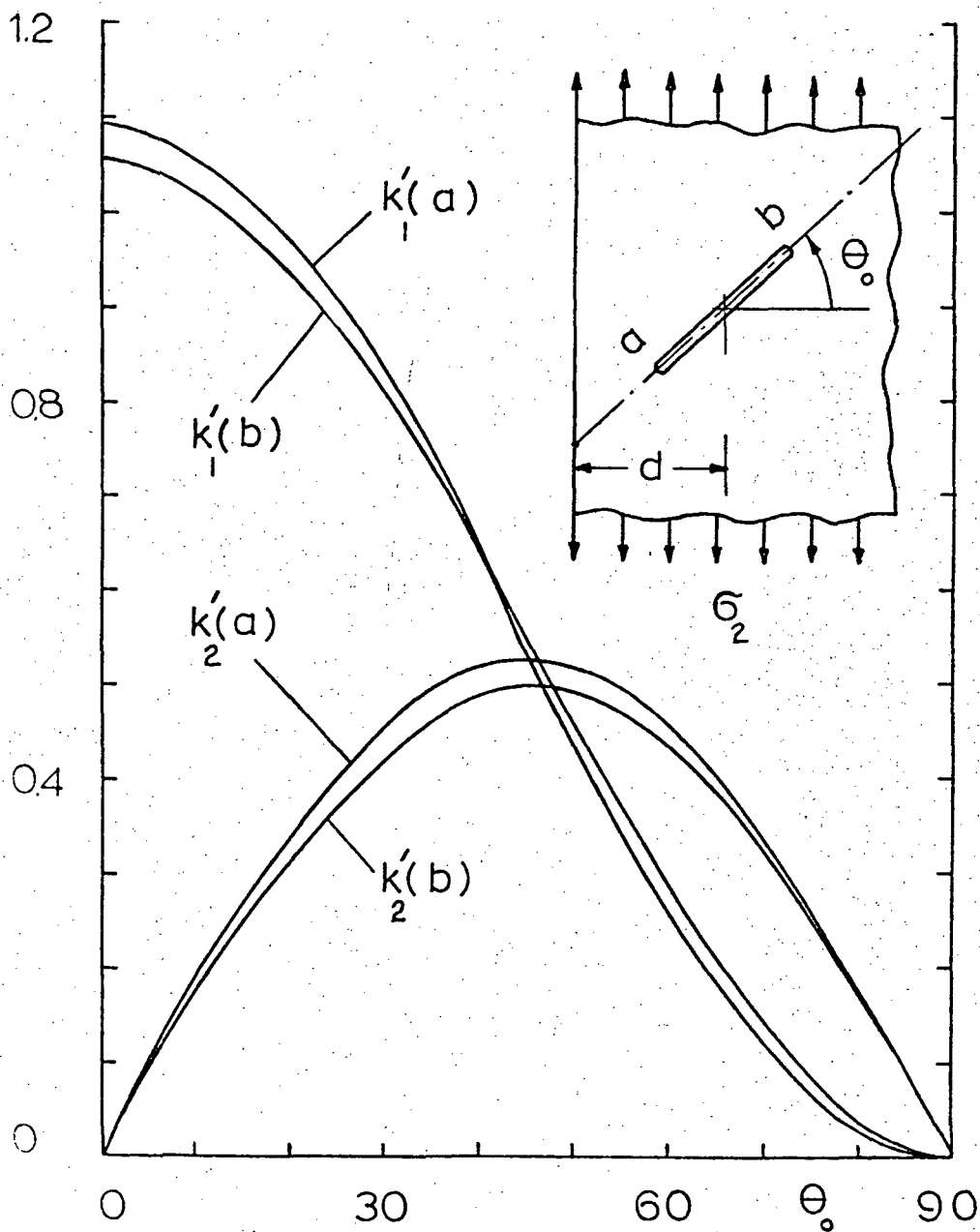


Figure 6. Stress intensity factor ratios in a half plane containing an arbitrarily oriented internal crack and loaded parallel to the free boundary ( $d = 2a_0 = b - a = \text{constant}$ ).

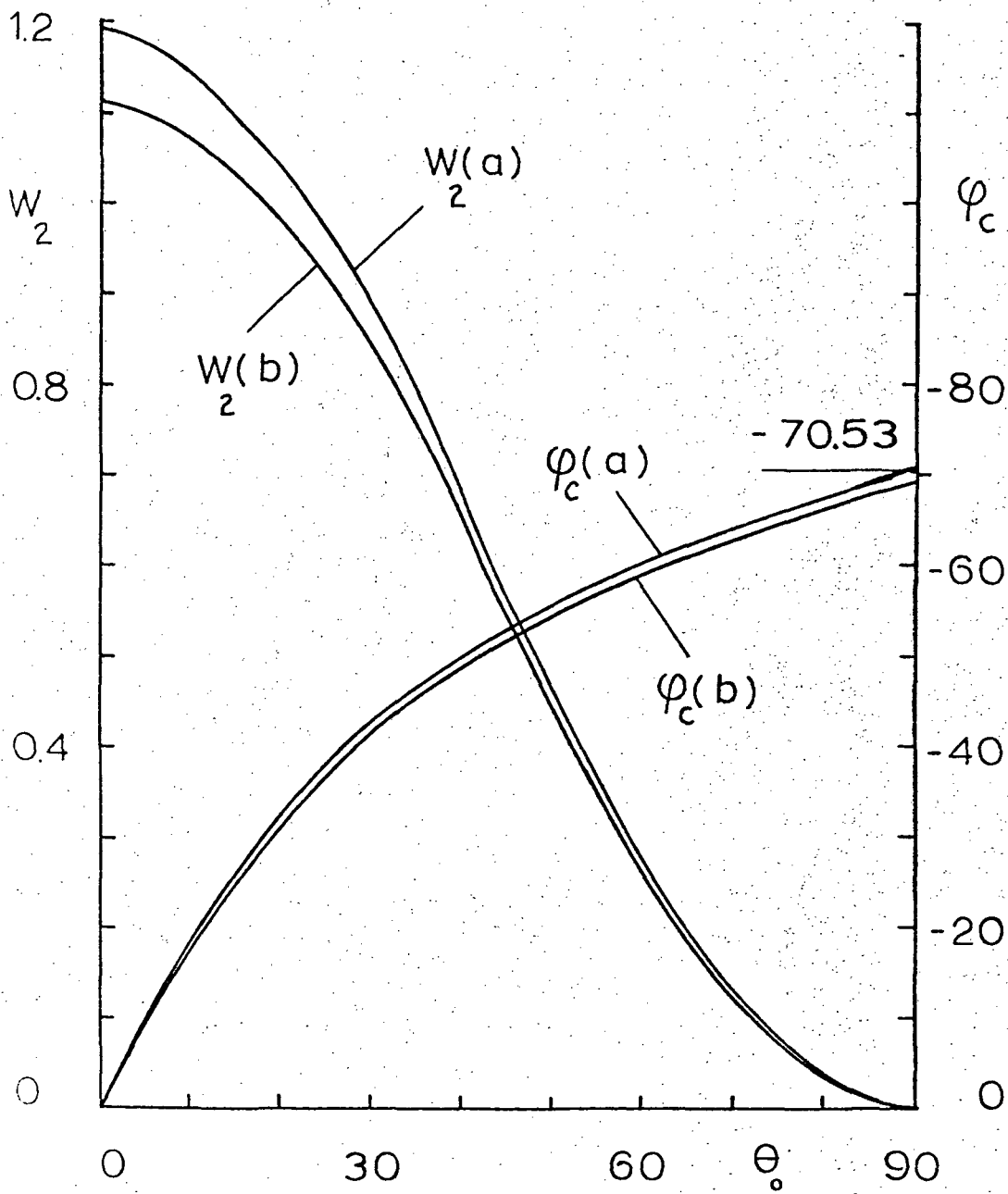


Figure 7.  $\phi_c$  and  $W_2$  for the half plane shown in Figure 6  
( $c = 2a_0 = b - a = \text{constant}$ ).

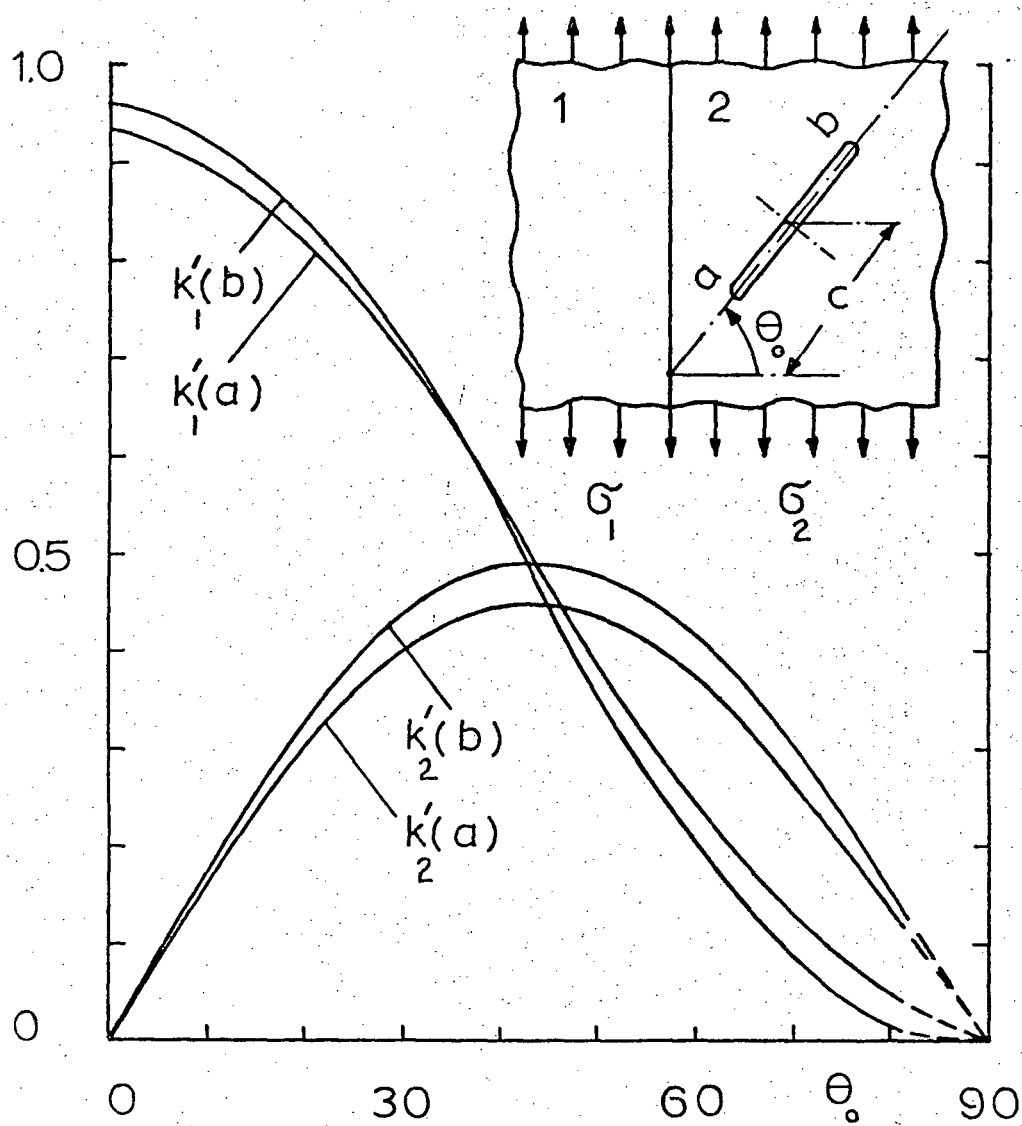


Figure 8. Stress intensity factor ratios in bonded half planes containing an arbitrarily oriented crack and loaded parallel to the interface ( $E_1/E_2 = 22.22$ ,  $\nu_1 = 0.3$ ,  $\nu_2 = 0.35$ ,  $c = 2a_0 = b - a = \text{constant}$ ).

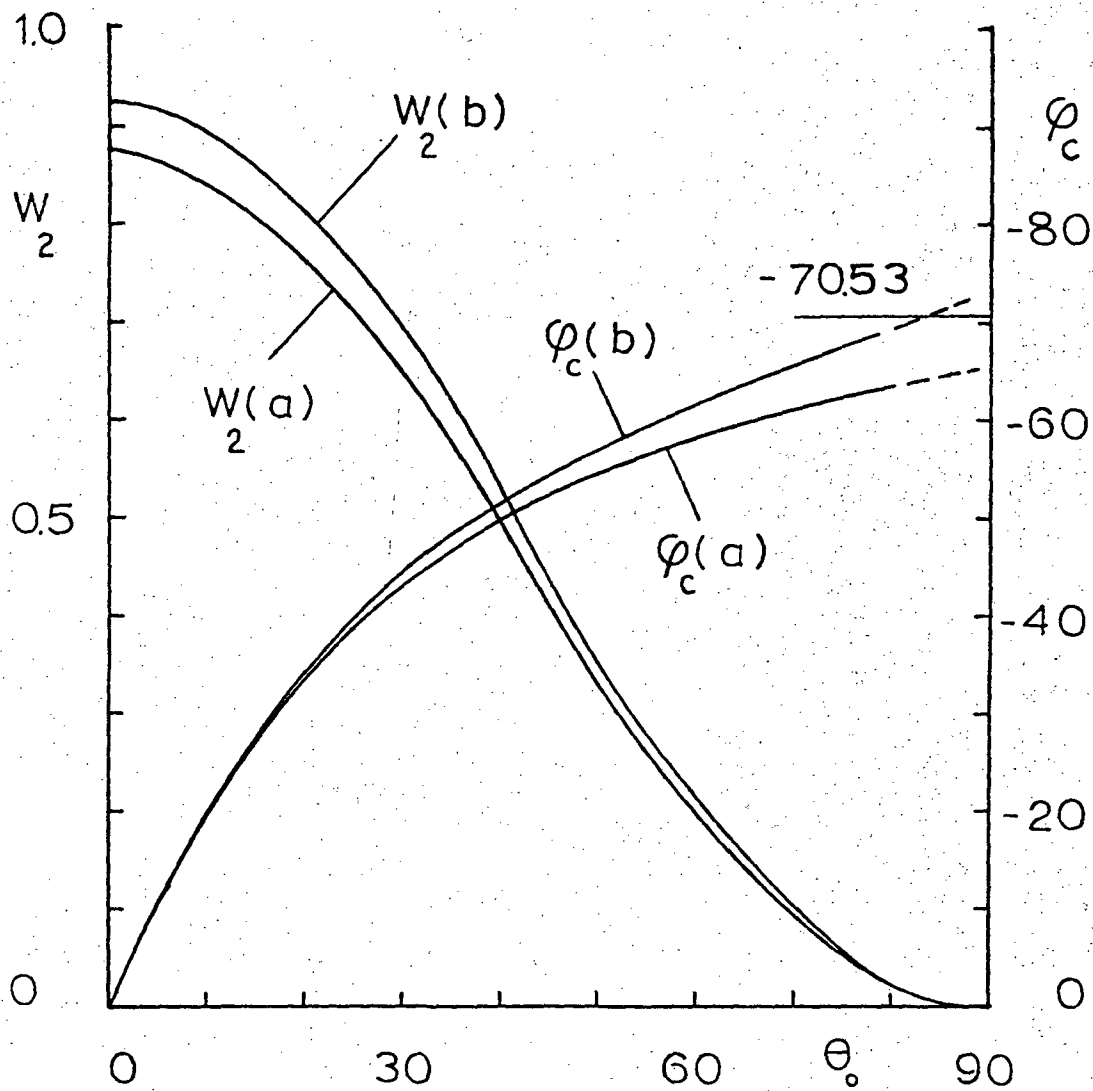


Figure 9.  $\phi_c$  and  $W_2$  for the bonded planes shown in Figure 8 ( $E_1/E_2 = 22.22$ ,  $\nu_1 = 0.3$ ,  $\nu_2 = 0.35$ ,  $c = 2a_0 = b - a = \text{constant}$ ).